

On smart optimization of blazed soft X-ray gratings

Werner Jark*

Elettra – Sincrotrone Trieste SCpA, SS 14 km 163.5 in AREA Science Park, Basovizza, 34149 Trieste, Italy.

*Correspondence e-mail: jark@elettra.eu

Received 15 February 2019

Accepted 26 March 2019

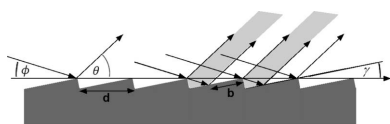
Edited by P. A. Pianetta, SLAC National Accelerator Laboratory, USA

Keywords: diffraction grating; soft X-rays; diffraction efficiency; soft X-ray monochromator.

The first attempts to calculate the diffraction efficiencies of gratings in the soft X-ray range were made on a scalar model. The results were simple analytical equations, that always severely overestimated the performance of real objects. In this respect, computer programs were found to be more successful, which rigorously consider all diffracted and refracted waves. Consequently soft X-ray gratings are presently optimized using these tools, which requires rather extensive calculations for any instrument optimization as general trends are not immediately obvious. Here it will be shown that the results of the rigorous calculations for gratings with blaze or sawtooth profile can be approximated rather well with a simple analytical equation. This equation contains three multiplicative factors, which deal independently with the effect of the reflectivity, the blaze angle and the groove density. This opens the possibility to initially ignore the effects of the blaze angle and thus to start an optimization in a very general way. Such optimization can be based on isorefectivity curves and it can then provide ‘blaze maximum efficiency maps’, *i.e.* simple images. In these latter images, one can identify directly the optimum parameters for a grating, *i.e.* the groove density providing best efficiency for a requested spectral resolving power. Only successively will the blaze angle have to be fixed. Its choice is then not the result of an extensive optimization process but of a simple calculation applied for the photon energy at which maximum efficiency performance is requested. The maps presented here are used for the optimization of a medium-resolving-power soft X-ray monochromator, which can scan the photon energy range 300–2000 eV.

1. Introduction

For the continuous tuning of the photon energy in the soft X-ray range with photon energies E from about 300 eV to beyond 3000 eV (photon wavelengths $0.4 \text{ nm} < \lambda < 4 \text{ nm}$; photon energy E and wavelength λ are related via $\lambda E = 1239.852 \text{ nm eV}$), monochromators employing diffraction gratings are almost exclusively used (Attwood, 1999). Presently the chosen parameters for the gratings are the result of systematic and lengthy calculations of their expected diffraction efficiencies with sophisticated software. The goal is to obtain the best possible diffraction efficiency for a proposed spectral resolution. The difficulties in the proper prediction arise from the need to operate the grating at very shallow angles of incidence below the critical angle for total reflection (Lukirskii *et al.*, 1963) and to consider properly the splitting of the incident intensity into several diffracted and refracted diffraction orders. The optimization could be very much shortened and be made more reliable if an independent tool was available that would readily provide a best parameter set for the start of the final optimization. However, such a tool is presently missing. Nevertheless, a few parameters can be decided on immediately, *e.g.* the groove shape. The intuitive expectation that a grating structure with a sawtooth profile, or a blazed profile as shown in Fig. 1, will provide the best effi-



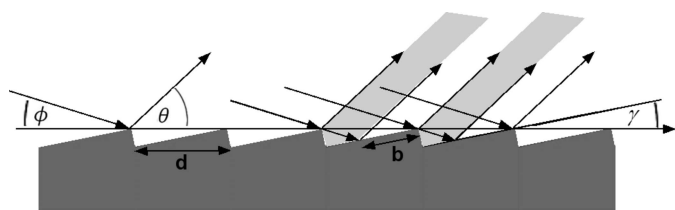


Figure 1

Diffraction of a radiation beam that strikes a diffraction grating with periodicity d with an angle of grazing incidence of ϕ , and which is diffracted by an angle of θ away from the surface. The situation is presented for a blazed grating with blaze angle γ . The illuminated area of width b is actively participating in the diffraction process. The radiation, being incident in the reversed orientation in the grey areas, cannot be diffracted by the common deflection angle.

ciency has been confirmed theoretically (Nevière & Flamand, 1980) and experimentally. When the optimization of grating monochromators for the soft X-ray range started, the choice fell to the use of such a profile to be operated in the vicinity of the blaze maximum, *i.e.* when the diffraction order of interest is specularly reflected at the grooves (*e.g.* Kunz *et al.*, 1968). The latter expectedly most favourable situation is presented in Fig. 1. In this case the angle of grazing incidence ϕ onto the grating surface is smaller than the grazing angle of diffraction θ ; and all incident radiation is intercepted at grazing incidence by shallow inclined grooves. In the reversed beam path, part of the incident intensity will hit the steeper part of the sawtooth, from where it cannot be diffracted into the desired direction. Also, the coating material can be chosen immediately, as a material possibly without any absorption structures in the projected tuning range will have to be favoured. Instead the remaining parameters, *i.e.* the groove periodicity of the grating and the inclination angle of the grooves, *i.e.* its blaze angle, require more systematic considerations and optimizations with appropriate computer programs. As a rule of thumb, one starts the optimization assuming that gratings with higher groove density can provide smaller spectral bandpass, while lower-density gratings provide better diffraction efficiency.

Here a tool will be discussed that readily indicates the optimum groove density, which will provide a requested spectral resolution with the highest possible diffraction efficiency. This tool is here used for the optimization of a soft X-ray monochromator for operation with medium spectral resolving power of 5000–10000 in the photon energy range 250–2000 eV at a diffraction-limited storage ring of the newest generation.

2. Operation parameters for soft X-ray monochromators

2.1. Plane-grating monochromators working in ‘fixed focus’ or blaze-maximum mode

As a first tool for finding appropriate operation parameters for diffraction gratings, Petersen (1982) introduced the so-called grating efficiency map, in which the ranges of grazing angles at which acceptable diffraction efficiencies had been

experimentally observed are plotted in relation to the monochromated wavelength. Petersen needed such a plot as he had optimized a monochromator for operation mostly in the off-blaze condition, and he wanted to quantify the sacrifice in diffraction efficiency for this particular operation. The reasoning for this operation mode will be discussed briefly here. The grating equation (see *e.g.* Hutley, 1982) for reflection gratings,

$$n\lambda = d(\cos \phi - \cos \theta), \quad (1)$$

requires that the monochromatization of a given wavelength λ by use of the diffraction of order n ($n \neq 0$) is made for differing angles of grazing incidence ϕ and of grazing diffraction θ . This equation is valid for periodic surface structures of any shape with periodicity d . In the present convention the order number is positive when a diffraction order falls between the incident beam and the beam being specularly reflected from the substrate (order $n = 0$). For $\theta \neq \phi$, the beam size will change in the diffraction process for all diffraction orders with the exception of the specularly reflected beam of order 0. As a consequence of this, the intrinsic beam divergence will also change (see, for example, Petersen, 1982). This will introduce aberrations to an incident uncollimated beam. For an observer downstream of the grating, the beam will then appear to be astigmatic as the new virtual position for the source in the dispersion direction will no longer coincide with its real position and thus with the unaltered position of the source in the orthogonal direction. It should be noted that the astigmatism problem can be overcome by collimating the beam prior to its dispersion; however, only at the expense of a flux reduction in an additional collimation mirror. Petersen (1982) wanted to avoid these losses and thus proposed an operation scheme in which the astigmatism, *i.e.* the position of the new virtual source, is kept constant during tuning. This so-called ‘fixed focus’ mode requires the beam size increase in the diffraction process to be kept constant. This is achieved by applying a constant ratio c_{ff} between the angles,

$$\sin \theta = c_{ff} \sin \phi, \quad (2)$$

with $c_{ff} > 1$ for the optical path as shown in Fig. 1. Instead, blaze maximum operation is achieved for a blaze angle γ in the condition

$$\phi + \gamma = \theta - \gamma. \quad (3)$$

Then in the ‘fixed focus’ mode the blaze maximum operation can be provided in only a single angular position. It should be noted at this point that for both operation modes one has to accompany the required grating rotation with a correlated rotation of a pre- or post-mirror, when the monochromated beam is to be stationary in angle and position. Now, in the off-blaze condition, one expects intuitively to observe losses in the diffraction efficiency and Petersen (1982) wanted to rapidly quantify them for his ‘fixed focus’ mode. At that time the grating quality could not be assured and thus he refrained from using already possible calculations for ideal profiles. Instead he decided to base his evaluation of the transmission

performance of his monochromator on published performance data for the grating efficiency. Petersen (1982) found that his chosen operation curve with $c_{\text{ff}} = 2.25$ for a grating with line density $p = 1220 \text{ mm}^{-1}$ (groove spacing $d = 825 \text{ nm}$) stayed inside the range for 50% of the maximum possible efficiency over the whole tuning range from $\lambda = 15 \text{ nm}$ down to below $\lambda = 0.8 \text{ nm}$ (photon energy range 80 eV to above 1500 eV). Jark (1988) later confirmed the validity of the maps with systematically measured efficiencies, which allowed him to present the data in the form of isoefficiency curves.

For the soft X-ray range indicated here only very grazing angles will be considered. It is then more convenient to use the small-angle approximations for the trigonometric functions. The grating equation then reads

$$n\lambda = \frac{d}{2}(\theta^2 - \phi^2). \quad (1)$$

From here on, the discussion will be restricted to the orders +1 and -1 to be diffracted from a sawtooth profile. In this case the optimum diffraction efficiency is found when the diffraction order of interest is specularly reflected at the inclined grooves. Intuitively one would have expected that Fig. 1 presents the condition for perfect diffraction into a single diffraction order. However, the reciprocity theorem requests the invariance of the diffraction efficiency upon exchange of the source and of the detector. Now, when the optical path is reversed compared with Fig. 1, then only part of the inclined sawtooth of width b can intercept and properly diffract the incident beam, while some intensity will be absorbed in the steeper part of the sawtooth. The undiffractable beam is incident in the light grey areas. In a short geometrical exercise it can be shown that the properly diffractable intensity is thus reduced by the factor

$$c' = \frac{\sin \phi \sin(\theta - \gamma)}{\sin \theta \sin(\phi + \gamma)}, \quad (4)$$

which for small angles becomes

$$c' = \frac{\phi(\theta - \gamma)}{\theta(\phi + \gamma)}. \quad (5)$$

The validity of the reciprocity theorem now requires applying this reduction factor also to the beam path shown in Fig. 1. This invariance request for the diffraction efficiency upon source and detector exchange was always used for validating programs for the calculation of the diffraction efficiencies, e.g. by Maystre & Petit (1976). Experimentally its validity was verified by Jark (1988). As far as the blaze maximum condition is concerned, Maystre & Petit (1976) established that the diffraction efficiency can be predicted with small error of the order of at most 10% with the simple relation

$$e_{\pm 1, \text{bm}} = R(\phi + \gamma) \frac{\phi}{\theta}. \quad (6)$$

Here, $R(\phi + \gamma)$ is the reflection coefficient for the inclined interface, for which $R(\phi + \gamma) = R(\theta - \gamma)$ holds, and the geometrical factor $c' = \phi/\theta$ is the factor from (5) applied to the blaze maximum condition. The angles in the ratio remain

unchanged, even though their meaning is reversed in the reversed beam path. In the latter path, θ is then referring to the angle of grazing incidence while ϕ is the angle of grazing diffraction. The symmetry required by the reciprocity theorem is then also respected in the calculations, when one considers the deflection angle $\phi + \theta$ as the relevant parameter for the reflectivity calculation. For all further considerations, here it will be attempted to express all relations as functions of this deflection angle. From equation (1') one finds readily that a minimum deflection angle exists for the diffraction, which is given by

$$(\phi + \theta)_{\text{min}} = \left(\frac{2\lambda}{d}\right)^{1/2}. \quad (7)$$

At blaze maximum, from (3) one obtains $\theta_{\text{bm}} = \phi + 2\gamma$, and by use of (1') one then obtains the working curve,

$$(\theta + \phi)_{\text{bm}} = \frac{\lambda}{d\gamma}. \quad (8)$$

By use of (7) and (8) one then finds a limitation for the tuning in the blaze maximum of

$$\lambda_{\text{min, bm}} \geq 2d\gamma^2. \quad (9)$$

For the earlier described 'fixed focus' mode (Petersen, 1982) with constant beam size increase in the diffraction process, one can approximate (2) by $\theta = c_{\text{ff}}\phi$ and one finds then

$$(\phi + \theta)_{\text{ff}} = \left(\frac{2\lambda}{d}\right)^{1/2} \left(\frac{c_{\text{ff}} + 1}{c_{\text{ff}} - 1}\right)^{1/2}. \quad (10)$$

For a given c_{ff} the corresponding deflection angle is then a multiple of the minimum possible deflection angle. Consequently no limitation exists in this mode for the tuning of the wavelength. In the latter case the variation of the deflection angle with wavelength λ follows a proportionality, $(\phi + \theta)_{\text{ff}} \propto \sqrt{\lambda}$, which is significantly smaller than at the blaze maximum, where one finds $(\phi + \theta)_{\text{bm}} \propto \lambda$. The here-discussed dependencies are presented in Fig. 2 for two example gratings with groove densities of 1200 mm^{-1} ($d = 833.3 \text{ nm}$), as chosen by Petersen (1982), and of 75 mm^{-1} ($d = 13,333 \text{ nm}$), which is a plausible lower limit for the groove density. For a grating with density 1200 mm^{-1} the data are shown at the top for two 'fixed focus' constants, $c_{\text{ff}} = 2.25$ and $c_{\text{ff}} = 1.5$, and for two blaze angles, $\gamma = 1.0^\circ$ and $\gamma = 1.5^\circ$. These numbers present the range that is mostly used in this type of monochromator (Petersen *et al.*, 1995). At the bottom only two working curves with $c_{\text{ff}} = 1.5$ and $\gamma = 0.25^\circ$ are presented. One can see, as mentioned earlier, that the 'fixed focus' monochromator operation mode will coincide with blaze maximum at only one particular photon energy. With the constant $c_{\text{ff}} = 2.25$ originally proposed by Petersen one finds, according to (10), $(\phi + \theta)_{\text{ff}, 2.25} = 1.61(\phi + \theta)_{\text{min}}$ and the ratio $(\phi + \theta)_{\text{ff}}/(\phi + \theta)_{\text{min}}$ increases with decreasing 'fixed focus' constant c_{ff} . Now for larger groove densities the range of inaccessible deflection angles extends to rather large angles, while the inaccessible range does not present a significant limitation for smaller groove densities. However, one needs to consider that the minimum deflection

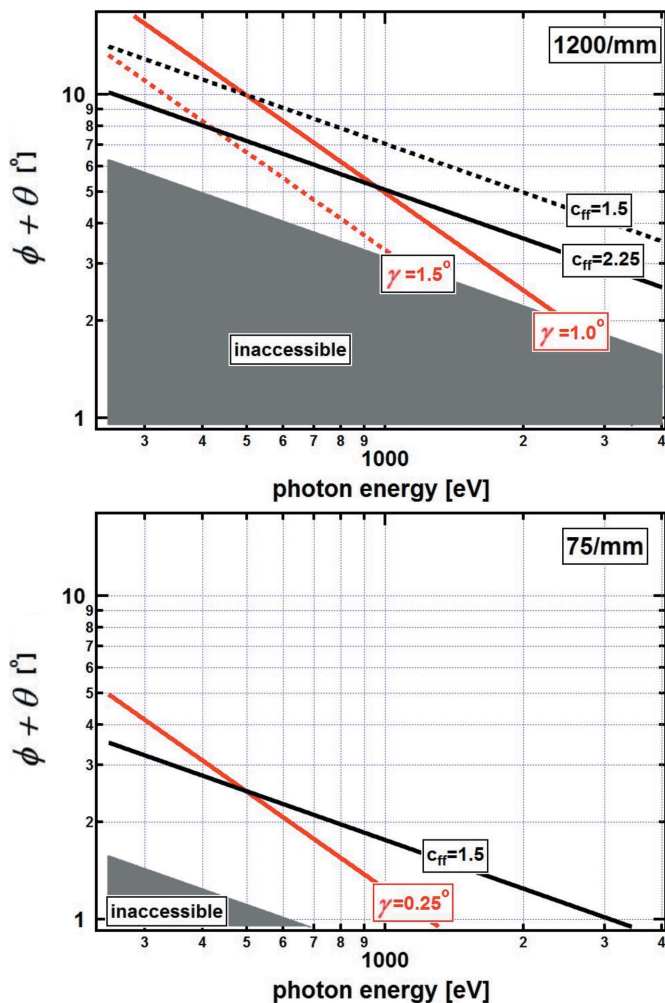


Figure 2 Working curves, *i.e.* the deflection angles $\phi + \theta$ at the grating, depending on the monochromated photon energy for different monochromator operation modes and grating groove densities. At the top, for a groove density of 1200 mm^{-1} ($d = 833.3 \text{ nm}$), the black curves refer to the ‘fixed focus’ operation according to (10) with the two different constants $c_{\text{ff}} = 2.25$ and $c_{\text{ff}} = 1.5$. The red curves refer to blaze maximum mode according to (8) with two blaze angles, $\gamma = 1.0^\circ$ and $\gamma = 1.5^\circ$. At the bottom, for a groove density of 75 mm^{-1} ($d = 13,333 \text{ nm}$), only curves for $c_{\text{ff}} = 1.5$ and a blaze angle of $\gamma = 0.25^\circ$ are presented. The grey area indicates the range of inaccessible deflection angles according to (7).

angle that can be operated in the related monochromator design (Riemer & Torge, 1983) or in modified versions for the ‘fixed focus’ operation proposed by Petersen (1982) will reasonably be limited to $(\phi + \theta) \geq 1.8^\circ$. Consequently the indicated operation of the grating with groove density 75 mm^{-1} is rather limited towards higher photon energies in both modes, *i.e.* in the ‘fixed focus’ and in the blaze maximum mode. An additional technological challenge lies in the very shallow blaze angles of only fractions of a degree, at which gratings with smaller groove densities will provide higher efficiencies. Heidemann *et al.* (2007) succeeded by use of reactive ion beam etching and the related significantly different etching rates for different materials to reduce the blaze angle in a grating with groove density of 300 mm^{-1} . A larger blaze angle of 2.8° in a mechanically ruled grating

structure in a gold layer could be transferred into the underlying silicon substrate with a final blaze angle of 0.1° . Voronov *et al.* (2018) achieved similar numbers more cost effectively starting with periodic structures produced by anisotropic etching into silicon.

2.2. Spectral resolving power

Now the primary performance parameter for the soft X-ray monochromator under discussion is in terms of spectral resolution. As far as this parameter is concerned, a routine operation with a spectral resolving power RP of the order of $(\lambda/\Delta\lambda) = 5000$ is projected for photon energies up to 2000 eV. The instrument should eventually also provide values of the order of $(\lambda/\Delta\lambda) = 10000$. An additional request is to keep the monochromatic beam cone behind the exit slit as circular as possible. Such a cone would then optimally illuminate the focusing optics, that is either rotationally symmetric or that is operated with square entrance apertures. An example of the first is focusing by use of Fresnel zone-plates (Attwood, 1999) and mono-capillaries (Voss *et al.*, 1992), while crossed Kirkpatrick–Baez mirror systems (Kirkpatrick & Baez, 1948) and particularly Montel mirrors (Montel, 1957) are examples of the latter situation. This latter request for a circular cone seems to match well with the fact that at diffraction-limited storage rings of the newest generation the radiation in the soft X-ray range will already be emitted into circular cones. However, according to (2) the diffraction at the grating will always alter the size of the incident beam in the dispersion direction. After diffraction with a ‘fixed focus’ constant c_{ff} , a beam of initially circular shape will have become a beam of elliptical shape with an aspect ratio between the ellipse axes in the dispersion and in the orthogonal direction of $S_{\text{disp}}/S_{\text{orth}} = c_{\text{ff}}$. A monochromator operation in the ‘fixed focus’ mode with the original constant $c_{\text{ff}} = 2.25$ is then not desirable; instead smaller constants of the order of $c_{\text{ff}} = 1.25$ could be accepted.

For the further discussion it will be assumed here that all reflection and diffraction processes take place aberrations-free, such that the phase space volume, *i.e.* the product of the source size and the beam cone opening angle, is preserved in the waists of the beam path. It will also be assumed that the incident beam is collimated by use of a collimation mirror. Then the ‘fixed focus’ mode can also be abandoned and a more flexible grating operation could be possible. In any case it will be assumed that the monochromator exit slit is always perfectly matched to the size of the monochromatic image.

The expected spectral resolution can be obtained from the derivative of the grating equation (1) or (1’) for the order $n = +1$, to which the discussion will be limited at this point,

$$\Delta\lambda = \frac{\partial}{\partial\theta} \lambda\Delta\theta \simeq d\theta\Delta\theta. \quad (11)$$

In the diffraction process one conserves the phase space volume when

$$\theta\Delta\theta = \phi\Delta\phi. \quad (12)$$

Then one can calculate directly the source-size-limited spectral resolution. For this purpose it will now be assumed that

the insertion device is operated slightly detuned, such that the maximum flux is intercepted in an aperture of finite size. According to Coisson (1988), in this case the σ parameter for the roughly Gaussian-shaped emission angle is given by $\sigma' = 1.3\sqrt{\lambda/D}$ in both directions. The source size is diffraction limited in the vertical direction with $\sigma_y = 0.15\sqrt{\lambda D}$; and the dispersion will thus be assumed to take place in this vertical direction. The corresponding full width at half-maximum values are then larger by a factor 2.35 than the σ values. Here the contribution from the electron beam size will be ignored.

The intrinsic angular spread in the beam due to the finite source size is then $\Delta\phi = 2.35\sigma/L$, where L is the distance of the grating from the source. One thus obtains, by use of (11) and (12), for the achievable spectral resolving power,

$$\left(\frac{\lambda}{\Delta\lambda}\right) = \frac{\lambda}{d\phi\Delta\phi} = 2.84 \frac{L}{d\phi} \sqrt{\frac{\lambda}{D}}. \quad (13)$$

In order to achieve this limit, it needs to be assured that the radiation cone illuminates a sufficient amount of lines at the grating, *i.e.* the number of illuminated lines needs to be larger than the requested spectral resolving power. This number of lines can be calculated from the size of the beam footprint at the grating via $\Delta L/d\phi$, and the final result

$$\frac{\Delta L}{d\phi} = 3.06 \frac{L}{d\phi} \sqrt{\frac{\lambda}{D}} \quad (14)$$

is just slightly larger than the achievable spectral resolution according to (13). This applies here in all cases and consequently this diffraction limit will be ignored in the further discussion. The angle of grazing incidence required to obtain a desired spectral resolving power ($\lambda/\Delta\lambda$) can be obtained from (13). It presents now a very interesting dependence in the form

$$\phi = \frac{2}{(\lambda/\Delta\lambda)} \frac{L}{\sqrt{dD}} \sqrt{\frac{2\lambda}{d}}. \quad (15)$$

Here $\sqrt{2\lambda/d}$ is the minimum deflection angle according to (7). Consequently the required angle of grazing incidence for a constant requested spectral resolving power ($\lambda/\Delta\lambda$) is a multiple of the minimum deflection angle. Now, when for a desired performance parameter the related angle of grazing incidence varies with the minimum deflection angle according to $\phi = A\sqrt{2\lambda/d}$ with constant A , then the related deflection angle to be obtained from $\phi + \theta = \phi + \sqrt{(2\lambda/d) + \phi^2}$ is also a multiple of the minimum deflection angle and it is given by $\phi + \theta = \sqrt{(2\lambda/d)}(A + \sqrt{A^2 + 1})$. Consequently the operation curves for constant spectral resolving power are at multiples of the minimum deflection angle. This was also the case for the ‘fixed focus’ operation curves. Then in any of the ‘fixed focus’ curves a constant spectral resolving power is provided, which can easily be calculated via

$$\left(\frac{\lambda}{\Delta\lambda}\right) = 2\sqrt{c^2 - 1} \frac{L}{\sqrt{dD}}. \quad (16)$$

Here the operation of the grating at a distance of $L = 22$ m from an undulator of length $D = 4.5$ m is considered. Similar

numbers will be used at presently projected diffraction-limited storage rings, and thus the results presented here could be almost directly applied in these cases. For differing parameters L' and D' , instead the achievable spectral resolving powers can simply be obtained by correcting the here-presented numbers according to (16) by the factor $(L'/22\text{ m})\sqrt{4.5\text{ m}/D'}$. For the two example gratings from Fig. 2 with groove densities of 1200 mm^{-1} and of 75 mm^{-1} , the related factors $2L/\sqrt{dD}$ in equation (15) lead to values of 22720 and of 5680, respectively. Consequently a spectral resolving power of 5000, as requested, can be achieved in both cases with convenient ‘fixed focus’ constants $c_{\text{ff}} < 1.3$.

2.3. Diffraction efficiency

2.3.1. Analytical calculations. At this point the achievable diffraction efficiencies will then have to be predicted for the optimum ‘fixed focus’ constants and the related groove densities. On the one hand, for this purpose one has available an analytical expression derived from a scalar approach by Sprague *et al.* (1955) and later by Lukirskii & Savinov (1963). Both groups derived an equation for the calculation of the diffraction efficiency for gratings in the form

$$e_n = R(\phi, \theta, \xi) S_n^2(\phi, \theta) G(\phi, \theta), \quad (17)$$

where R is a reflection coefficient depending on the angles ϕ and θ and on the refraction angle into the substrate ξ . S is the structure factor derived for the order n in analogy to the Fraunhofer diffraction from a multislit system,

$$S_n = \frac{\sin\{(\pi b/\lambda)[\cos(\phi + \gamma) - \cos(\theta_n - \gamma)]\}}{(\pi b/\lambda)[\cos(\phi + \gamma) - \cos(\theta_n - \gamma)]}, \quad (18)$$

with

$$b = d \left[\cos \gamma - \frac{\sin \gamma}{\tan(\phi + \gamma)} \right] = d \frac{\sin \phi}{\sin(\phi + \gamma)}. \quad (19)$$

The geometrical factor G is derived by Sprague *et al.* (1955) to be $G = \sin \theta / \sin \phi$, while Lukirskii & Savinov (1963) derive for a sawtooth profile grating the factor $G = \sin(\theta - \gamma) / \sin(\phi + \gamma)$. The authors of both studies were not aware of the validity of the reciprocity theorem. In the study by Lukirskii & Savinov (1963) the respective correction factor $\sin \phi / \sin \theta$ is thus missing, and the correct form for G should have been as given above in (4). Then measured data were always falling significantly behind the expectations, which were erroneously too optimistic. Consequently this scalar approach was abandoned rather early for any instrument optimization.

2.3.2. Rigorous calculations with the differential method. As far as a better agreement between predictions and experiment is concerned, the differential method for the calculation of the diffraction efficiencies as presented by Nevière *et al.* (1974) was finally successful. This rigorous approach thus became the tool used for the optimization of the grating parameters in the design stage for monochromators (*e.g.* Schäfers, 2008; Boots *et al.*, 2013). Now this code and its modification can treat perfect grating profiles, but

can also take into account distortions in the profiles (Boots *et al.*, 2013).

2.3.3. Analytical approximation of rigorously calculated diffraction efficiencies. In the present study, we now attempt to return to an analytical expression that would provide diffraction efficiencies in agreement with the rigorous Neviere code (Nevière *et al.*, 1974). This would very much help to accelerate the systematic optimization as a designer would then be able to use simpler and readily available software for a first optimization. In this initial design stage it is acceptable to assume a perfect grating profile. In fact, any possible imperfections should in the first place reduce the relative diffraction efficiency but should not affect the optimum working point for any wavelength. Obviously such an analytical expression needs to predict the diffraction efficiency in the blaze maximum as given in (6). Plausibly it should also contain the structure factor as presented in (18) and part or all of the geometrical factor G as presented in (4) or (5). In a systematic comparison with the Neviere code for the perfect profile it was then assumed that the reflection coefficient can be used in the form $R(\phi + \theta)$ not only in the blaze maximum condition but in general. For the commonly used coating of gold these latter coefficients are now presented colour-coded in Fig. 3. These coefficients were calculated by use of the Center for X-ray Optics Database (2019). The most convenient form of the plot is as isoreflectivity curves, *i.e.* as a reflectivity map depending on the photon energy and on the deflection angle. When now the rigorously calculated diffraction efficiency e_{rig} for a given grating periodicity d and blaze angle γ is divided by the corresponding reflection coefficient $R(\phi + \theta)$ from Fig. 3, then the resultant ratio $e_{\text{rig}}/R(\phi + \theta)$ agrees for $\theta > \gamma$ with little error, of the order of 10% or less, with the product of the structure factor according to (18) and the simplified geometrical loss factor ϕ/θ ,

$$\frac{e_{\text{rig}}}{R(\phi + \theta)} = S_{n=1}^2 \frac{\phi}{\theta}. \quad (20)$$

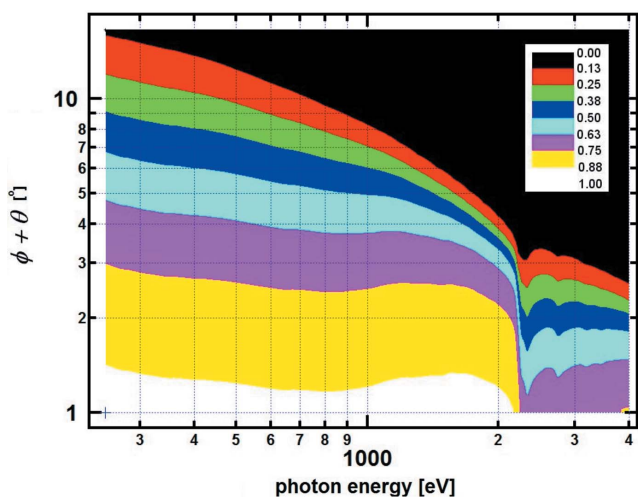


Figure 3 Isoreflectivity curves for a gold coating in a plot of deflection angle $\phi + \theta$ versus photon energy. The reflectivities corresponding to the borders between different colours are indicated in the colour bar, which covers the range of reflectivities $0 < R < 1$.

The latter simple loss factor ϕ/θ , which was shown by Maystre & Petit (1976) to be applicable for the calculation of the blaze maximum diffraction efficiency for the order $n = +1$, is identical to the reciprocal of the ‘fixed focus’ constant, *i.e.* with $1/c_{\text{ff}}$.

3. Discussion

3.1. Grating efficiency maps

An additional important result for further discussion is the observation that the product of the geometrical factors on the right-hand side of equation (20) is bell-shaped. The maximum occurs always very close to the blaze maximum condition as given by (3). The width of these curves varies with photon energy and blaze angle. For the purpose of this study, it is now important to recognize that the diffraction efficiency can be calculated by use of three multiplicative factors,

$$e = R(\phi + \theta) S_{n=1}^2 \frac{\phi}{\theta}. \quad (21)$$

In this equation the contributions from the reflectivity, the grating blaze angle and the groove density and geometry separate into independent factors. At blaze maximum, the bell-shaped structure factor is $S_{n=1}^2 = 1$. The width in the deflection angle and in the photon energy, in which $S_{n=1}^2$ is at least 0.5, can be estimated via $\{[\sin(B)]/B\}^2 = 0.5$, which is achieved for $B = 0.44\pi$. Then one finds by use of the small-angle approximation that at a given photon energy the efficiently diffracting interval of deflection angles is given by

$$\frac{(\theta + \phi)_{\text{max}}}{(\theta + \phi)_{\text{min}}} = \left[1 + \frac{B}{\pi} \frac{\phi_1 + \gamma}{\phi_1} \right] / \left[1 - \frac{B}{\pi} \frac{\phi_2 + \gamma}{\phi_2} \right], \quad (22)$$

while the corresponding photon energy interval for a given deflection angle is given by the same ratio,

$$\frac{E_{\text{max}}}{E_{\text{min}}} = \left[1 + \frac{B}{\pi} \frac{\phi_1 + \gamma}{\phi_1} \right] / \left[1 - \frac{B}{\pi} \frac{\phi_2 + \gamma}{\phi_2} \right]. \quad (23)$$

Here the indices 1 and 2 refer to the angles of grazing incidence at the upper and at the lower limit of the intervals, respectively. Both ratios are at least $[1 + 0.44]/[1 - 0.44] = 2.57$, when the blaze angle can be ignored in comparison with the angles of grazing incidence, and they are larger otherwise. The extremes for the minimum ratio are then at about 0.55 and 1.45 of the deflection angle or photon energy corresponding to blaze maximum, respectively.

The latter ratio 1.45 is important for the applicability of equation (21). This equation was tested in the soft X-ray range between photon energies of 300 eV and 4000 eV, *i.e.* in the window chosen in all figures. In this range it estimates the diffraction efficiency for the first order, but also for the second order, with similarly small error (<10%) compared with the rigorous calculations. It was found to be applicable for the first order also in the EUV range 30–300 eV. In all cases the simple predictions become unreliable when the working curve involves deflection angles in excess of 1.45-fold the working curve for blaze maximum. In these areas the structure factor $S_{n=1}^2$ decreases very rapidly towards a local minimum. This

can produce significant discrepancies between the rigorous calculations and the simple predictions by use of (21). However, this has little effect on the optimization in which one will always point to high efficiencies. Similar observations are not made for smaller deflection angles. The reflectivity factor $R(\phi + \theta)$ in (21) can only be applied in the case of a sawtooth with apex angle 90° and a thick coating. In fact, equation (21) cannot account for any interference in a thin coating or for interferences which are caused by intensity being transmitted through the tips of the profile. Only a rigorous approach can properly account for these effects. Likewise only the rigorous approach will permit to interpret measured efficiencies when the grating profile is defective, *e.g.* when it presents rounded tips or a varying groove inclination.

Now, as far as any ‘fixed focus’ working curve is concerned, the structure factor $S_{n=1}^2$ remains larger than 0.5 between 0.35 times and 2.1 times the photon energy at which the blaze maximum condition is found. This permits a relative operation in this mode to at least $E_{\max} = 6E_{\min}$. This scanning limit covers already two-thirds of the presented window in Figs. 2 and 3, *e.g.* the scanning could cover efficiently the photon energy range 300–1800 eV, while it is not limited to this range. Consequently the here-requested slightly larger tuning range can be covered in ‘fixed focus’ mode with a single grating; and the just discussed feasibility of efficient tuning in rather large photon energy intervals in this ‘fixed focus’ mode invites to initially ignore completely the blaze angle in the optimization. As it is only contained in the structure factor in (21), one would then calculate the efficiency for $S_{n=1}^2 = 1$ by use of $e = R(\phi + \theta)(\phi/\theta)$. This is identical to (6) for the calculation of the diffraction efficiency of a blazed grating in blaze maximum. Consequently when one now plots for a given groove density the diffraction efficiencies according to (6) in analogy to Fig. 3 as isoefficiency curves depending on photon energy and on deflection angle, the result can be called a ‘blaze maximum efficiency map’. It can now be used as a powerful tool for the further optimization of the grating in a monochromator. Without consideration of the exact groove profile these maps allow one to compare directly the ultimately possible performance by use of gratings with varying groove densities. The reflection coefficient for the commonly used coating material gold can be taken from Fig. 3. Then Fig. 4 presents the ‘blaze maximum efficiency maps’ for the three different groove densities (from top to bottom) of 1200 mm^{-1} , 300 mm^{-1} and 75 mm^{-1} . The most obvious observation is a significant variation of the maximum diffraction efficiency with groove density. On the one hand the changes are rather insignificant in the isoefficiency curves towards the upper right. In fact here the isoefficiency lines follow very much the behaviour of the isoreflectivity lines in Fig. 3. On the other hand, towards the lower left the shape of the isoefficiency curves is dominated by the correction factor $\phi/\theta = 1/c_{\text{gr}}$, which leads to increasing geometrical losses when the inaccessible angular range is approached. Fig. 2 points out already that the reduced inaccessible angular ranges for smaller groove densities make the areas of larger reflectivities, as of Fig. 3, available when such gratings are used. Consequently the diffraction efficiency

increases with decreasing groove density and simultaneously also the efficiently diffracting angular range increases. These observations are in line with past practical and theoretical experiences. The maximum diffraction efficiency obtainable in the blaze maximum condition is presented at the top of Fig. 5

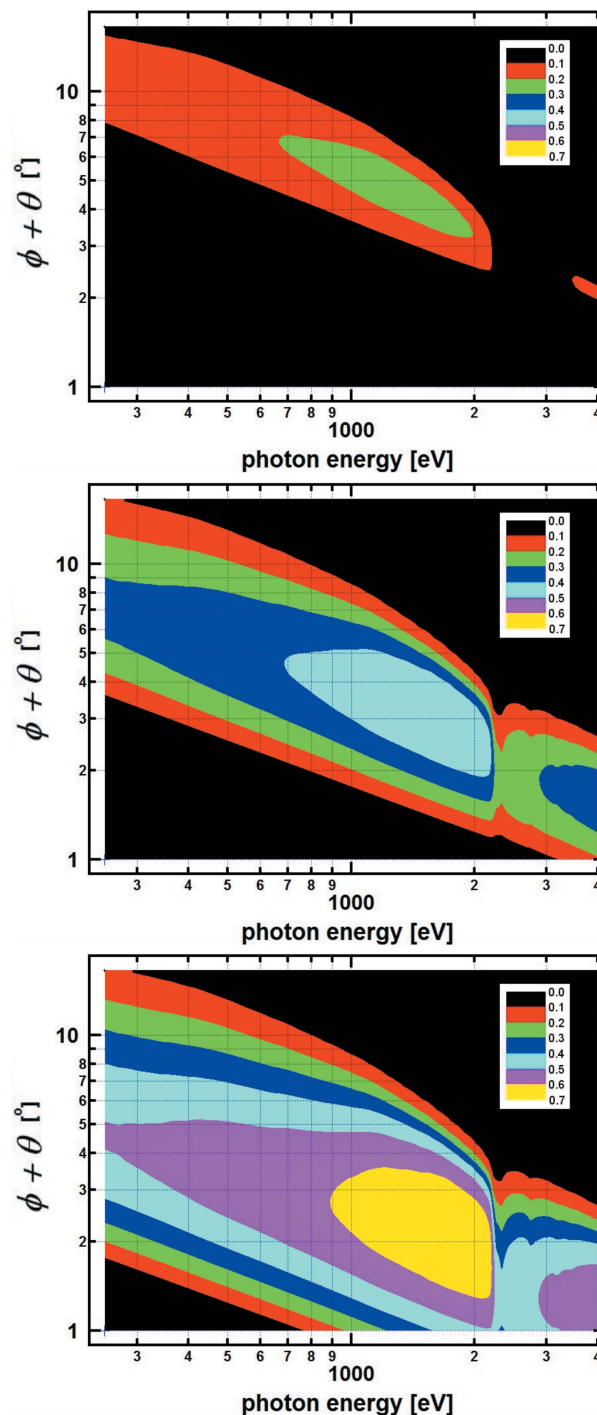


Figure 4 ‘Blaze maximum grating efficiency maps’, *i.e.* isoefficiency curves according to (6), for gold-coated blazed gratings in a plot of deflection angle $\phi + \theta$ versus photon energy for different groove densities (from top to bottom) of 1200 mm^{-1} , 300 mm^{-1} and 75 mm^{-1} . The efficiencies corresponding to the borders between different colours are indicated in the colour bar, which covers the range of efficiencies in blaze maximum $0 < e < 0.7$.

for a photon energy of 1580 eV, around which the best performance is found. The variation in the presented range of groove densities $50 \text{ mm}^{-1} \dots 1200 \text{ mm}^{-1}$ is here more than a factor of three.

Comparison of these ‘blaze maximum efficiency maps’ from Fig. 4 and of the isorefectivity curves from Fig. 3 with the grating operation curves in Fig. 2 shows some interesting behaviour. In the optimization stage of early grating monochromators for operation at blaze maximum (Kunz *et al.*, 1968) it was argued that the blaze maximum operation curves would follow well the critical angle behaviour of the metal coatings. This would be the case when absorption in the coating material can be neglected. However, this is not the case for a gold coating in the soft X-ray range. In fact the absorption reduces the reflectivity particularly towards smaller photon energies. As a result, when compared with the operation curves in Fig. 2, the isorefectivity curves do not really follow

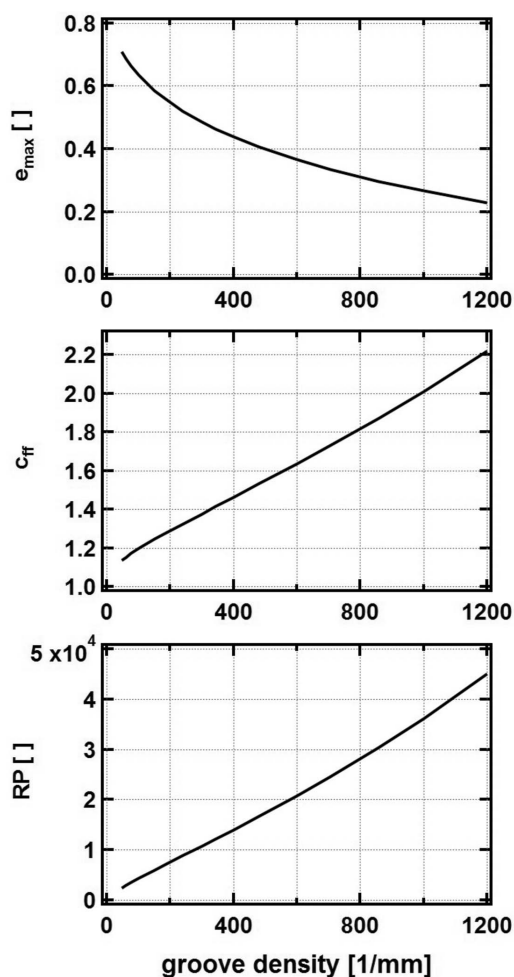


Figure 5
 Top: maximum diffraction efficiency e_{max} depending on the groove density of blazed gratings at a photon energy of 1580 eV, where the ‘blaze maximum grating efficiency maps’ in Fig. 4 indicate best diffraction performance. Center: ‘fixed focus’ constants c_{ff} depending on the groove density of blazed gratings for the monochromator operation, which will provide maximum diffraction efficiency. Bottom: spectral resolving power RP depending on the groove density, which a monochromator will provide when operated with the ‘fixed focus’ constants c_{ff} from the centre figure at 22 m from a 4.5 m-long undulator at a diffraction-limited storage ring.

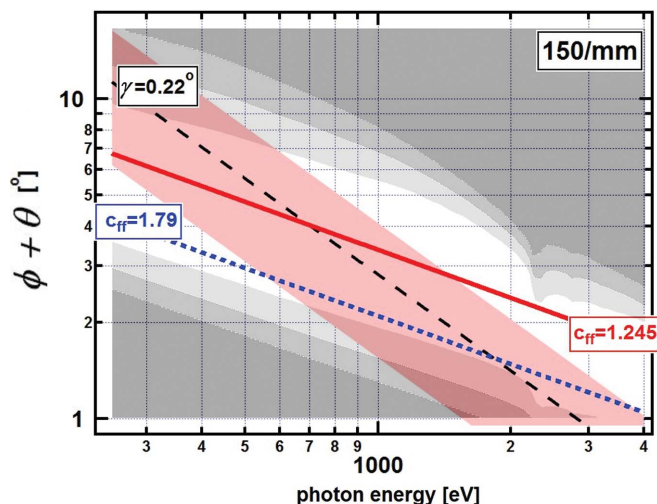
the steeper inclination of the blaze maximum curves but more the smaller inclination of the ‘fixed focus’ curves. This latter inclination is also dominating the ‘blaze maximum efficiency curves’ for the gratings in Fig. 4. Then, as far as the grating is concerned, operation in the ‘fixed focus’ mode seems to be also the most favourable operation mode efficiency-wise. According to equation (10) one can then assign an ‘optimum’ ‘fixed focus’ constant to each groove density. The diffraction efficiency is maximum on the related operation curves, and the corresponding spectral resolving power for the chosen source is constant. The dependence of both the c_{ff} constant and the spectral resolving power RP on the groove density is presented in Fig. 5 for operation below the gold *M*-absorption edges, *i.e.* for photon energies $< 2200 \text{ eV}$. Both the c_{ff} constants and the related spectral resolving powers increase roughly linearly with increasing groove density. As far as the operation of a 1200 mm^{-1} grating, as chosen by Petersen with a ‘fixed focus’ constant of $c_{\text{ff}} = 2.25$, is concerned, this is now found to be an optimum choice for tuning at photon energies below 2200 eV. For the optimization of the monochromator transmission the plots invite choosing the smallest groove density as the most efficient solution, which is compatible with the requested spectral resolution. One should note that the wider ‘blaze maximum efficiency curves’ for smaller groove densities provide more flexibility for a possible variation of c_{ff} . Once the wavelength λ at which the monochromator is to provide optimum performance at blaze maximum is established, the final choice of the blaze angle can be made simply by use of

$$\gamma = \frac{1}{2} \left(\frac{2\lambda}{d} \right)^{1/2} \left(\frac{c_{\text{ff}} - 1}{c_{\text{ff}} + 1} \right)^{1/2} \quad (24)$$

Then at least 50% of the optimally available diffraction efficiency according to Fig. 4 would be provided between $0.35 \times$ and $2.1 \times$ of the related photon energy.

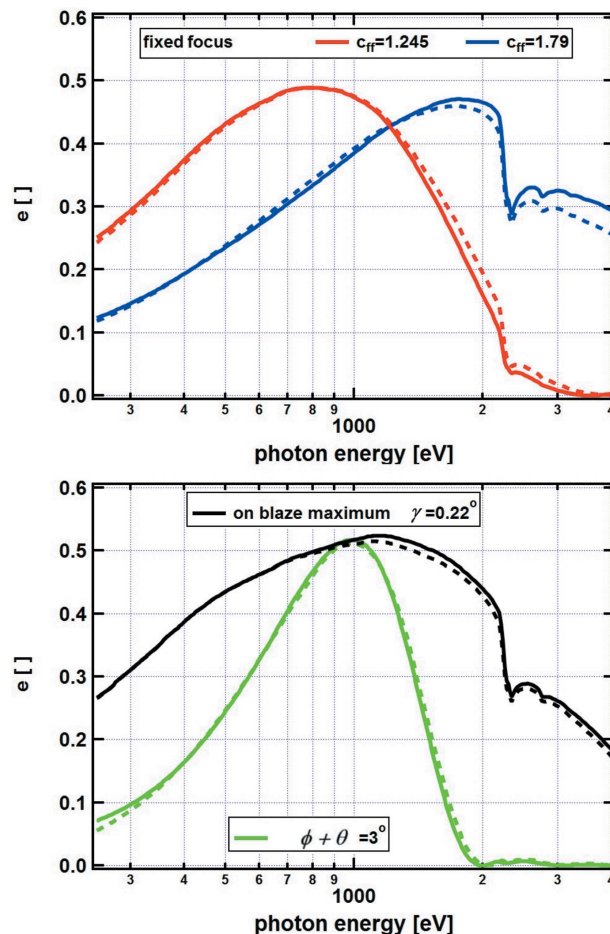
3.2. Monochromator optimization for spectral resolution and transmission

For the proposed monochromator with requested spectral resolution of $\text{RP} = 5000$ the optimum groove density is then 150 mm^{-1} or smaller. In this case for 150 mm^{-1} a spectral resolving power RP of slightly better than 5000 can be achieved with high diffraction efficiency and with a convenient ‘fixed focus’ constant of $c_{\text{ff}} = 1.245$. The related operation curve (red line) is presented in Fig. 6 in comparison with a normalized ‘blaze maximum grating efficiency map’, which is presented in grey scale for photon energies below 2200 eV. The latter map presents in white the angular ranges in which $> 75\%$ of the maximum diffraction efficiency is provided. Likewise light grey stands for $> 50\%$, darker grey for $> 25\%$ and dark grey for $< 25\%$. In this case the twofold-increased spectral resolving power of around $\text{RP} = 10000$ can be obtained with $c_{\text{ff}} = 1.79$ (dashed blue curve), which can still be provided with relatively high efficiency ($> 75\%$). The photon energy for the blaze maximum operation in standard mode was chosen to be 700 eV ($\lambda = 1.77 \text{ nm}$). The related working curve is then plotted in Fig. 6 as a dashed black line, around


Figure 6

Comparison of monochromator operation curves with the normalized 'blaze maximum grating efficiency map' for a gold-coated blazed grating with groove density of 150 mm^{-1} . The grey scale refers to zones of equal relative performance for blazed gratings. In the white area more than 75% of the maximum possible diffraction efficiency is achieved, while in the dark grey areas the relative performance is less than 25% of maximum performance. In the lighter grey area $>50\%$ is provided, while in the darker grey areas at least $>25\%$ is available. The solid red and the dashed blue line refer to the 'fixed focus' operation according to (10) with the two constants $c_{\text{ff}} = 1.245$ and $c_{\text{ff}} = 1.79$. The dashed black line refers to the operation at blaze maximum according to (8) for the chosen blaze angle of $\gamma = 0.22^\circ$. At the borders of the light red areas the diffraction efficiency of the chosen blazed grating will have decayed to about 50% of the maximum.

which the pink area indicates the angular range in which at least 50% of the maximum achievable diffraction efficiency can be provided. The blaze maximum for the higher spectral resolving power of $\text{RP} = 10000$ is then found for a larger photon energy of almost 2000 eV. However, the related working curve still points to only a moderate loss of 50% in the diffraction efficiency, when the grating is tuned to 700 eV. The angular width of the 'efficiency curves' permits to tune the monochromator in the entire projected range also at blaze maximum condition. Fig. 7 (top) now compares the calculated diffraction efficiencies by use of equation (21) (solid lines) and by use of the rigorous code (dashed lines) for the indicated chosen parameters for both 'fixed focus' operation curves. For comparison purposes also the calculation for blaze maximum is presented (black curves) at the bottom of Fig. 7, as is the result for a constant deflection angle of $(\phi + \theta) = 3^\circ$ (green curves). The results from equation (21) agree mostly to within 10% with the results from the rigorous calculations. The discrepancy exceeds 10% only for 'fixed focus' operation with $c_{\text{ff}} = 1.245$ at photon energies around 2000 eV. As discussed earlier and presented in Fig. 6, in this range the structure factor decreases rapidly to values <0.5 , which results in lower efficiencies which can then be predicted rather unreliably by use of (21). Otherwise all calculations confirm the expectations as they would be derived by use of Fig. 6. At lower energies, $c_{\text{ff}} = 1.245$ provides best efficiency, about twofold better than $c_{\text{ff}} = 1.79$. At the upper limit for the photon energy, $c_{\text{ff}} = 1.79$ performs about twofold better. The blaze maximum


Figure 7

Comparison of the first-order diffraction efficiency e calculated by use of the here-proposed equation (21) (solid lines) and by use of the rigorous calculation code proposed by Nevière *et al.* (1974) (dashed lines) depending on the photon energy for a grating with a gold coating, a groove density of 150 mm^{-1} and a blaze angle of $\gamma = 0.22^\circ$. In the top figure the data are presented for the 'fixed focus' operation with constants $c_{\text{ff}} = 1.245$ (red curves) and $c_{\text{ff}} = 1.79$ (blue curves), while in the bottom figure the black curves refer to the performance in blaze maximum mode and the green curves refer to the diffraction efficiency for a fixed deflection angle of $\phi + \theta = 3^\circ$.

mode would actually always provide the best transmission. However, in this case the 'fixed focus' constant is increasing in a scan with increasing photon energy, which then leads to variations, *i.e.* increases, in the beam cross sections and in the spectral resolving power. When the grating is operated at fixed deflection angle, then the efficient tuning range is reduced to about a factor of 2.5–3 in photon energy, as indicated earlier.

For stability reasons, in a monochromator one would prefer to operate the plane-mirror–plane-grating pair with parallel beam offset for the monochromated radiation. Consequently the beam deflection angles at the pre-mirror and at the grating will have to be identical. Then the higher diffraction efficiency provided by gratings with lower groove density is achieved in combination with higher reflectivity as the pre-mirror is operated at correspondingly shallower deflection angles. These more favourable angular regimes become inaccessible when gratings with larger groove densities are used. The

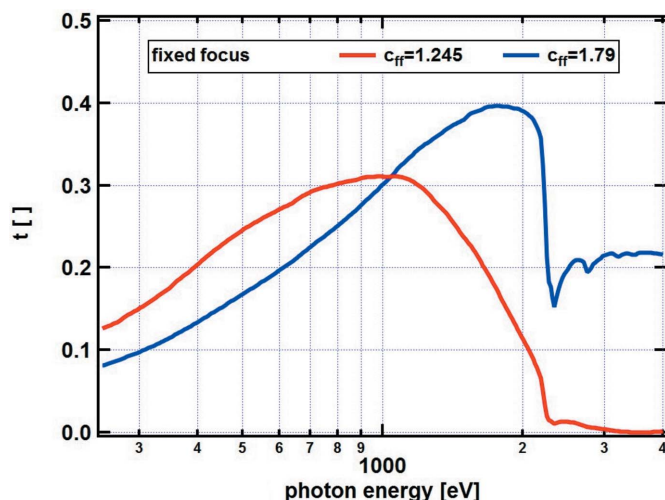


Figure 8 Comparison of the transmission t of a combination of plane-mirror–plane-grating depending on the photon energy, when both components are gold coated and the monochromatic beam is exiting parallel to the incident beam. The data are calculated by use of (25). The grating has a groove density of 150 mm^{-1} and a blaze angle of $\gamma = 0.22^\circ$ and for the operation mode ‘fixed focus’ with constants $c_{ff} = 1.245$ (red line) and $c_{ff} = 1.79$ (blue line).

transmission t through such a combination of ideal components is then given by

$$t = R^2(\phi + \theta) S_{n=1}^2 \frac{\phi}{\theta}. \quad (25)$$

The calculated results by use of (25) for the two ‘fixed focus’ modes from Fig. 7 (top) are presented in Fig. 8. One can see that the steeper angles, which need to be operated at the mirror for the smaller c_{ff} constant, reduce the instrument transmission in the entire working range more significantly than the smaller angles, which are realized in combination with larger c_{ff} constant.

As the relevant parameter in the presentation of the isoefficiency curves in Fig. 4 is the deflection angle, these maps are also valid for the operation of the grating in the reversed orientation compared with Fig. 1 with the order $n = -1$. It can be shown that the achievable spectral resolving power in this situation is smaller compared with the results discussed here by the factor $1/c_{ff}$. This result favours then the use of the normal orientation, as in this case a reduced spectral resolving power can be achieved with a decreased groove density and thus with an advantageously increasing transmission. The normal orientation is also more resistant to an incident heat load, as the steeper side of the sawtooth remains hidden from it. On the other hand, the grating for operation in the reversed orientation can be shorter, which may be an advantage in some particular cases.

4. Conclusion

‘Blaze maximum grating efficiency maps’ have been presented for gratings with gold coating and with significantly varying groove densities. It is proposed that these maps can be used as universal curves for finding readily the optimum parameters

for the operation of blazed gratings in monochromators for the soft X-ray range even though the blaze angle is not considered. In fact, once a decision has been made on the projected spectral scanning range and on the required spectral resolution of a monochromator, the present data indicate readily the grating groove density that will provide the best diffraction efficiency in combination with it. The spectral resolving power is constant when the monochromator is operated in ‘fixed focus’ mode at an undulator source at a diffraction-limited storage ring. It is found that efficient diffraction can be achieved in the same mode. Then the optimum ‘fixed focus’ constant varies with the groove density of the grating and depends on the coating material. The blaze angle will be chosen only successively. In terms of diffraction efficiency, 50% of optimum performance can be achieved in energy intervals around the blaze maximum condition in which the upper energy limit is six-fold the lower energy limit. This needs to be considered for the choice of the photon energy at which maximum efficiency at blaze maximum operation is projected. An optimization is discussed for a monochromator to be operated with maximum transmission and with a spectral resolving power of 5000 in the soft X-ray range with photon energies between 250 eV and 2200 eV. It is found that this can be achieved with a grating with a groove density of 150 mm^{-1} and a blaze angle of $\gamma = 0.22^\circ$. The spectral resolving power is constant when the grating is operated in the ‘fixed focus’ mode with a ‘fixed focus’ constant of $c_{ff} = 1.245$. The grating can also be operated efficiently in the blaze maximum mode. It will then provide better efficiency, but also smaller bandpass at the upper energy limit. The presented parameter choice was made by use of the universal curves, and the expected performance was then discussed with simple approximations. The predicted relative performance was then found to agree with the predictions by the simple model and by rigorous calculations.

Acknowledgements

The author would like to thank very much Dr F. Schaefer from the Helmholtz-Zentrum Berlin (HZB/BESSY-II) for the possibility to use the *REFLEC* program, which he developed, for some of the presented calculations.

References

Attwood, D. (1999). *Soft X-rays and Extreme Ultraviolet Radiation: Principles and Applications*. Cambridge University Press.
 Boots, M., Muir, D. & Moewes, A. (2013). *J. Synchrotron Rad.* **20**, 272–285.
 Center for X-ray Optics Database (2019). *Mirror Reflectivity*, http://henke.lbl.gov/optical_constants/mirror2.html.
 Coisson, R. (1988). *Opt. Eng.* **27**, 273250.
 Heidemann, K. F., Nelles, B. & Lenke, R. (2007). *AIP Conf. Proc.* **879**, 485–488.
 Hutley, M. (1982). *Diffraction Gratings: Techniques of Physics*. New York: Academic Press.
 Jark, W. (1988). *Nucl. Instrum. Methods Phys. Res. A*, **266**, 414–421.
 Kirkpatrick, P. & Baez, A. V. (1948). *J. Opt. Soc. Am.* **38**, 766–774.
 Kunz, C., Haensel, R. & Sonntag, B. (1968). *J. Opt. Soc. Am.* **58**, 1415–1416.

- Lukirskii, A. P. & Savinov, E. P. (1963). *Opt. Spectrosc.* **14**, 147–151.
- Lukirskii, A. P., Savinov, E. P. & Shepelev, Y. P. (1963). *Opt. Spectrosc.* **15**, 290–293.
- Maystre, D. & Petit, R. (1976). *Nouv. Rev. Opt.* **7**, 165–180.
- Montel, M. (1957). *X-ray Microscopy and Microradiography*, pp. 177–185. New York: Academic Press.
- Nevière, M. & Flamand, J. (1980). *Nucl. Instrum. Methods*, **172**, 273–279.
- Nevière, M., Vincent, P. & Petit, R. (1974). *Nouv. Rev. Opt.* **5**, 65–77.
- Petersen, H. (1982). *Opt. Commun.* **40**, 402–406.
- Petersen, H., Jung, C., Hellwig, C., Peatman, W. B. & Gudat, W. (1995). *Rev. Sci. Instrum.* **66**, 1–14.
- Riemer, F. & Torge, R. (1983). *Nucl. Instrum. Methods Phys. Res.* **208**, 313–314.
- Schäfers, F. (2008). *The BESSY Raytrace Program RAY*, in *Springer Series in Optical Science*, Vol 137, *Modern Developments in X-ray and Neutron Optics*, edited by A. Erko, M. Idir, T. Krist & A. G. Michette. Springer, Heidelberg: Berlin.
- Sprague, G., Tomboulia, D. H. & Bedo, D. E. (1955). *J. Opt. Soc. Am.* **45**, 756–761.
- Voronov, D. L., Gullikson, E. M. & Padmore, H. A. (2018). *Opt. Express*, **26**, 22011–22018.
- Voss, J., Dadras, H., Kunz, C., Moewes, A., Roy, G., Sievers, H., Storzjohann, I. & Wongel, H. (1992). *J. X-ray Sci. Technol.* **3**, 85–108.